3D Hydrodynamics in the Upper Human Bronchial Tree: Interplay Between Geometry and Flow Distribution.

B. Mauroy[1),2)]

[1)] Centre de Mathématiques et de Leurs Applications, Ecole Normale Supérieure de Cachan, 61 avenue du Président Wilson, 94235 Cachan, France
[2)] UPRES EA 2397, Université Paris 6, Paris, France

Summary. Uniform flow distribution in a symmetric volume can be realized through a symmetric branched tree. It is shown however, by 3D numerical simulation of the Navier-Stokes equations, that the flow partitioning can be highly sensitive to deviations from exact symmetry if inertial effects are present. The flow asymmetry is quantified and found to depend on the Reynolds number. Moreover, for a given Reynolds number, we show that the flow distribution depends on the aspect ratio of the branching elements as well as their angular arrangement. Our results indicate that physiological variability should be severely restricted in order to ensure adequate fluid distribution through a tree. Time-dependant simulations have also been performed and have shown that inspiration and expiration flows are both subject to inertial effects but with completely different velocities structures.

1 Introduction

The purpose of the bronchial tree is to bring air from outside into the gas exchange units, the acini. Its structure can be approximately described by a dichotomical tree of seventeen generations, each seventeenth generation branch being connected to an acinus. Moreover, this geometry is not passive and air is brought into and out of the tree by dilatation and contraction of the acini, which act like little pumps. This phenomenon is called ventilation. Even though the acini are very small, their large number implies that air velocity reaches, at rest, around 1 $m.s^{-1}$ in the trachea [1] (the Reynolds number is close to 1200). This shows that inertial effects exist, even at rest, in the first generations of the lung and that they can play a non negligible role in flow repartition. Hence, the goal of this work was to understand how important these effects are. Because lung is ventilated, it has been also interesting to check inertia consequences during each ventilation regimes, i.e. during inspiration and during expiration.

To answer these questions, numerical simulations have been performed in different lung models. Theoretical models, with remarkable symmetric properties, have first been used, for they are easier to interpret. Stationary simulations of inspiratory state have been performed in three generations trees with varying parameters [2]. The parameters are the length to diameter ratio of branches, the angle between the two successive branching planes and the Reynolds number. The stationary results have then been confirmed with time-dependant simulations (which need much larger simulation time). These calculations have shown that, because of inertia, flow properties are dependant of geometry, even if the tree is built to fill symmetric volumes at low flow rates. Hence, the well known M-shape [3] appears during inspiration. It creates a sensitive difference in flow or pressure repartition at exits and, without an active regulation, variability could lead to high inhomogeneities in the lung. The time dependant simulations have also shown that tree response is completely different in terms of flow profiles whether the tree inspires or whether it expires. In our simulations, expiratory inertial effects are observed to be more adapted to the symmetry properties of the tree than inspiratory ones.

These results have then been confirmed in a more realistic model based on H. Kitaoka bronchial tree model [4]. Moreover, the lower parts of the lung, which are the most demanding in terms of flow, are favoured by inertial effects. This indicates a probable adaptation of lung geometry to inspiratory inertial effects.

2 Models and Methods

2.1 Geometries

The models consist in dichotomical trees, each branch being cylindrical. Each branching is symmetric, i.e. daughter branches are identical. Moreover, a mother branch and its daughter branches are always in the same plane, as observed in the real lung. See Fig. 1 for tree examples. For time dependant simulations, enlarged pistons have been added to each exit to simulate a pumping coming from the base of the tree, like in real lungs, see right tree on Fig. 1.

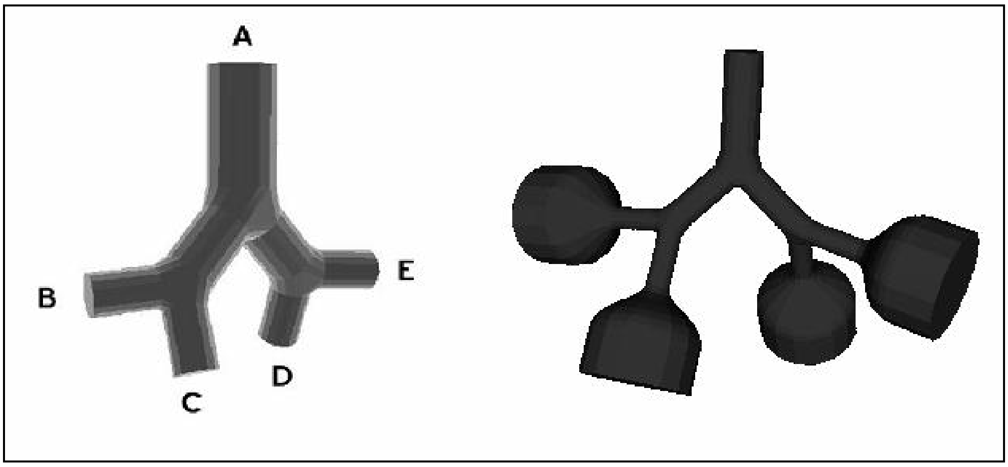

Figure 1: Examples of geometrical models used in numerical simulations. Left: a tree for stationary simulations. Right: a tree for time dependant simulations, with piston structures at each exit.

The models are discretized with meshes consisted in around 300 000 tetraedra. Most of the simulations use three generations trees, for this is a reasonable choice in term of elements size and calculation times. Note that meshes are built with the software SIMAIL from Simulog.

2.2 Equations

Air fluid mechanics taking place in the lung are modelized with full Navier-Stokes equations, the non linear term being the source of inertial effects. These equations can be written, with u and p respectively representing air velocity and pressure:

$$\begin{cases} \frac{\partial u}{\partial t} + (u.\nabla)u - \frac{\mu}{\rho}\Delta u + \frac{\nabla p}{\rho} = 0 \\ div(u) = 0 \end{cases}$$

ρ represents air density ($\rho=1.18\ kg.m^{-3}$) and μ is air viscosity ($\mu=1.785\ .\ 10^{-5} kg.m^{-1}.s^{-1}$).

Boundary conditions must also be defined to complete the mathematical problem. Non slip conditions ($u=0$) have been put everywhere, except at entry (**A** on Fig. 1) and at exits (**B**, **C**, **D** and **E** on Fig. 1). The choice of boundary type for these last surfaces is not easy, for real conditions in lungs are unknown. Hence, there is always an ambiguity between imposing velocity or pressure (or even mixed conditions). Comparison between both types of conditions has been done in the stationary case. It has shown that there exists a duality between velocity and pressure relatively to the tree response to inertia [5].

Numerical simulations of Navier-Stokes equations have been performed with the software N3S from Simulog.

3 Stationary Simulations (Inspiration)

The following results have been published in [2] and [5] in collaboration with B. Sapoval, M. Filoche and J.S. Andrade Jr.

3.1 Dependence on Geometry

An example of the models used in this section is shown on the left part of Fig. 1. Two geometrical parameters have been checked: the length to diameter ratio (L/D with values 2.5, 3, 3.5 and 4) and the angle between the two branching planes (α ranging from $0°$ to $180°$ with steps of $15°$, the reference angle $\alpha=0°$ corresponds to a coplanar tree). In the real lung, L/D mean is close to 3 and α mean to $90°$. See reference [2] for more details.

The first set of simulations uses a parabolic velocity profile at inlet (**A** in Fig. 1) and an imposed pressure P_0 with homogenous Neumann conditions at outlets (**B**, **C**, **D** and **E** on Fig. 1). Note the symmetry of the exit boundary conditions. We are interested in the flow difference at outlets. Firstly, the problem symmetry leads to $\Phi_B = \Phi_E$ and $\Phi_C = \Phi_D$. The flow asymmetry Σ_F can then be defined relatively to one side of the geometry:

$$\Sigma_F(\alpha, \frac{L}{D}) = \left| \frac{\Phi_B - \Phi_C}{\Phi_B + \Phi_C} \right|$$

In the case where inertia can be neglected, the asymmetry Σ_F will always be 0 in the conditions of this section. Hence, this number is a representation of inertial effects in the trees.

The results are given on Fig. 2. First, increasing L/D leads to a reduction of flow asymmetry because the flow breaking created by branching has more length to recover an homogenous profile. For α angle, it is interesting to see that there exists a point ($\alpha=90°$) leading to a perfect repartition of the flow into the outlets ($\Sigma_F=0$), this is a consequence of symmetrical properties of the geometry for this particular *α*. However, a small change of *α* around this value leads to a quick increase of asymmetry. Hence, if such structures are stacked together, some outlets will receive a large quantity of flow while others will receive very little flow [2]. At the limit, this could lead to a multifractal repartition of the flow [6]. This type of phenomena cannot exist in the lung and a flow regulation should prevent such inhomogeneities.

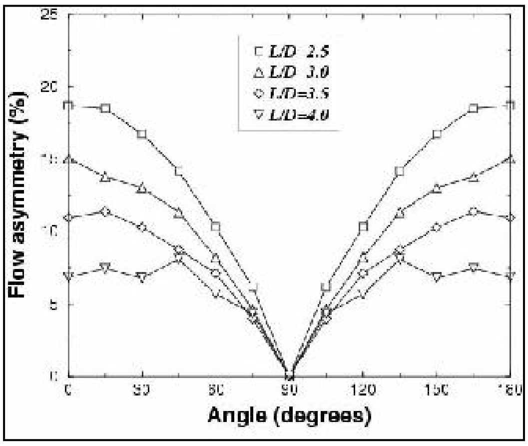

Figure 2: Dependence of the flow asymmetry Σ_F relative to the angle α. The different curves represent different values of *L/D*. Note that $\alpha=90°$ is surrounded with steep variations of Σ_F, and that increasing *L/D* decreases the flow asymmetry.

The sensibility of angle variation around $\alpha=90°$ is a consequence of the typical velocity profile created by inertial effects after the first bifurcation: the M-shape [3], as shown on the right of Fig. 3. On this figure, velocity is represented in grey levels and is decreasing from dark to white. Flow repartition at outlets is the result of how the second bifurcation is splitting the M-shape. Hence, bifurcating with $\alpha=90°$ leads to capture the flow according to the axial symmetry of the M-shape, see Fig. 3. Because of the velocity repartition, a small change from *90°* corresponds to remove a large quantity of flow from one side and to add it to the other side. This explains the sensitivity of Σ_F around $\alpha=90°$ [2].

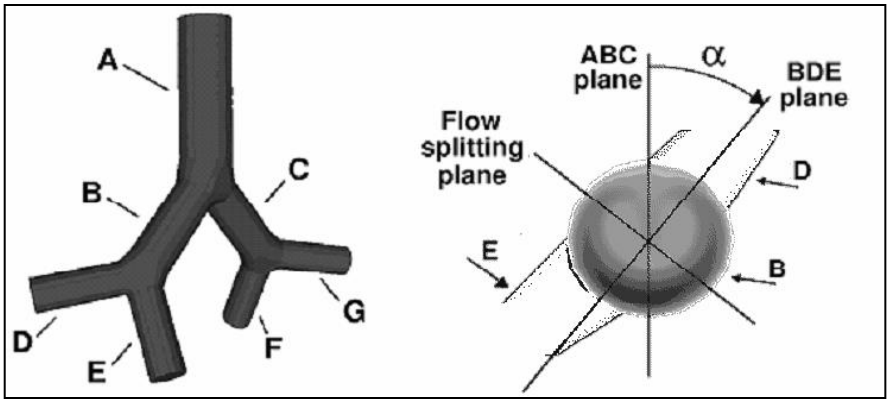

Figure 3: The sensitivity around $\alpha=90°$ is a consequence of the typical velocity profile called M-shape (right). This is a result of the way outlets (D and E) are capturing the flow from the M-shape.

The second set of simulations has been performed with pressure imposed condition at entry and flow imposed conditions at exits [5]. Now, consequences of inertia are measured through pressure differences between outlets. Pressure asymmetry is defined by:

$$\Sigma_P(\alpha) = \left| \frac{P_B - P_C}{P_B + P_C} \right|$$

Results for angle dependence (with *L/D=3*) are shown on Fig. 4. As for the previous boundary conditions type, there exists a sensitivity relatively to angle variations around *90°*. Differences between the two cases are noticeable only for angles close to *0°* and *180°*, however such angle values are not present in human lungs. Hence, like in the first simulations set, a phenomena leading to inhomogeneities in term of pressure repartition can be deduced from these simulations. Thus, an active regulation is needed to obtain homogenous properties of the flow.

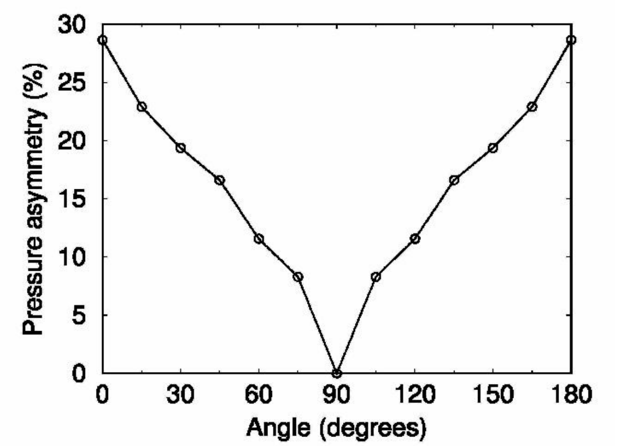

Figure 4: Dependence of pressure asymmetry relative to the angle α. The sensitivity around $\alpha=90°$ is always present for this second type of boundary conditions.

3.2 Dependence on Reynolds Number

The dependence of asymmetry relative to Reynolds number will give an approximate generation from which inertial effects can be neglected. Simulations have been performed on two different geometries for different Reynolds (from *120* to *1200* with steps of *120*). Results are shown on the curve on Fig. 5. The asymmetry increased quickly until reaching a Reynolds number of around *360*. Then its variations are small and a plateau appears. These effects are visible through the M-shape: it becomes much more homogenous as the Reynolds number is decreasing, see right part of Fig. 5. To very low Reynolds numbers, the M-shape is a set of concentric circles corresponding to a Poiseuille profile. If we assume that inertial effects are negligible when flow asymmetry is smaller than *2%*, then we can obtain an approximate generation below which inertia can be neglected. At rest, this generation is the sixth one.

Hence, flow equations in the lower bronchial tree can be simplified, authorizing analytic studies, see [6].

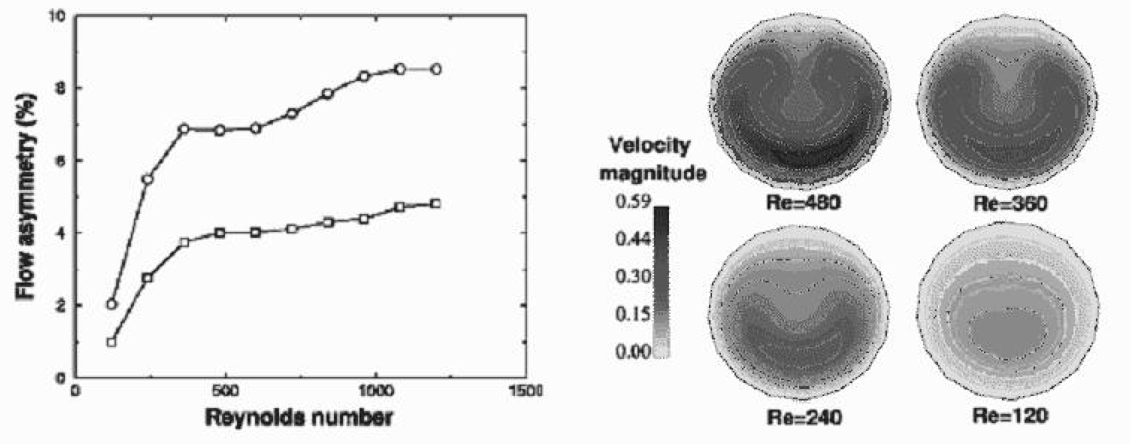

Figure 5: Left: Dependence of flow asymmetry relative to Reynolds number for two geometries: *L/D=3*, *α=75°* (squares) and *α=60°* (circles). The asymmetry is first increasing quickly, and then it reaches a plateau. Right: M-shape for different Reynolds numbers. When the Reynolds is low, the M-shape becomes more homogenous.

4 Time Dependant Simulations

In the preceding section, time influence has been neglected. It has been shown that inertia has important consequence on a stationary inspiratory flow. It will be shown here that its influence will be different whether the tree is inspiring or expiring. During the inspiratory phase, inertial effects are similar to those observed in stationary mode with the typical M-shape profile. During the expiratory phase, the flow structure is better adapted to geometry. This work is the result of collaborations with B. Sapoval, M. Filoche, T. Similowski and C. Straus.

4.1 Two Generations Trees

First, a simple two generations model has been used to highlight the consequences of inertia on flow structure, see Fig. 6. As for all time-dependent simulations, piston-like structures have been added at each exit to simulate lung pumping. The ventilation cycle has been modelised with sinusoidal oscillations of pistons (with a 5 seconds period). This is an approximation of the real lung ventilation which has an inspiration time of around 2 seconds and an expiration time of around 3 seconds. At entry, the pressure has been imposed.

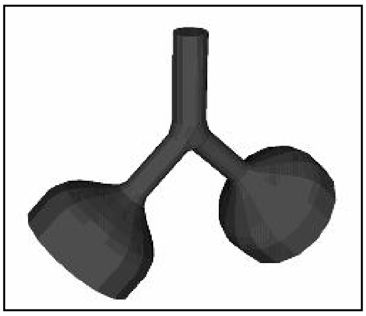

Figure 6: Two generations geometry used in this section. The piston-like structures at exits simulate lung pumping.

Velocity profiles in both generations and during both inspiratory and expiratory phases are shown on Fig. 7 (highest speed time for a *600* Reynolds number). As expected, a M-shape is present at inspiration in the second generation. It is also interesting to note that although pressure has been imposed at entry, its velocity profile is a Poiseuille profile. During expiration, however, inertial effects are mostly present in the first generation, where two high velocities peaks appear. First, it is remarkable that velocity level lines are symmetrical relatively to the centre of the section. Secondly, measurements have shown that [7]

1- inspiration dissipates *10%* more energy through viscous effects than expiration (data for a *1200* Reynolds number at entry, close to rest regime).
2- expiration flow profile in the first generation is much closer to Poiseuille profile than inspiration flow in the second generation.

Hence in our model, expiration leads to more homogenous flow than expiration. Such results could have important consequences in term of lung design understanding [7].

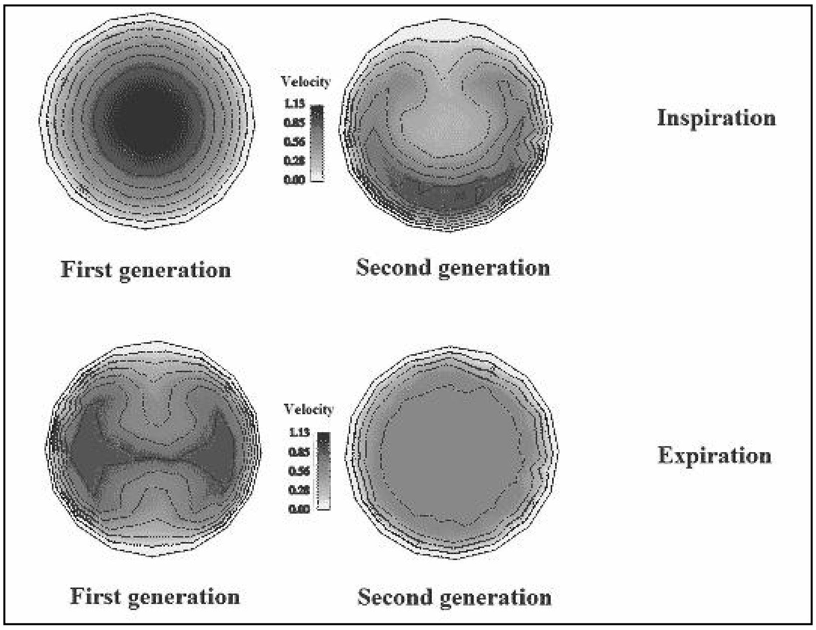

Figure 7: Velocity profiles in both generations of a two generations tree. Top: cuts during inspiration. Bottom: cuts during expiration. The dissymmetry between the two ventilation regimes is noteworthy.

4.2 Three Generations Tree

M-shape existence in time-dependant simulations shows that the structure of the flow is still the consequence of inertial effects. Thus, asymmetry in flow properties also exists and it is interesting to study its repartition during ventilation. In this section, air velocity is calculated in a three generations tree, with structures at outlets acting as pistons (oscillating in a sinusoidal way with 5 seconds period), see Fig. 8. Because flow is imposed at exists, pressure asymmetry has been chosen to represent inertia (in the same way than section **3**).

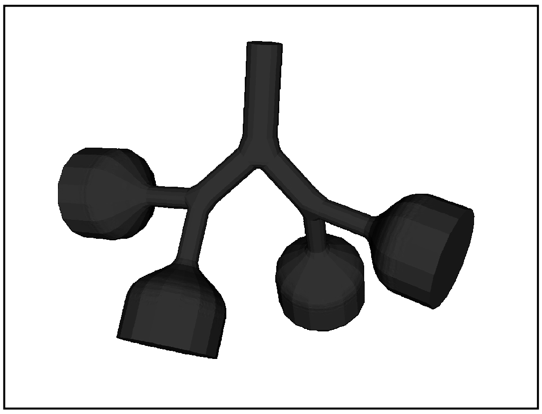

Figure 8: Three generations tree used in this section. Outlet structures act as pistons to ventilate the geometry.

Figure 9 shows the pressure asymmetry evolution during a respiratory cycle. Pressures are measured at piston's top. The differences between inspiration (0 – 2.5 seconds) and expiration (2.5 – 5 seconds) are remarkable. The pressures in the different pistons need to be different to compensate inertia only during high velocity inspiration times. Note that for low velocity times, there is very little inertia and hence there is nothing to compensate. However during expiration, the piston's pressures are exactly the same for the four tree-ends. Thus, inertia leads to non homogenous flow properties only during inspiration. This fact is coherent with the preceding remarks on flow structure in the section **4.1**. Hence our models show that inspiring in a tree is more complex than expiring.

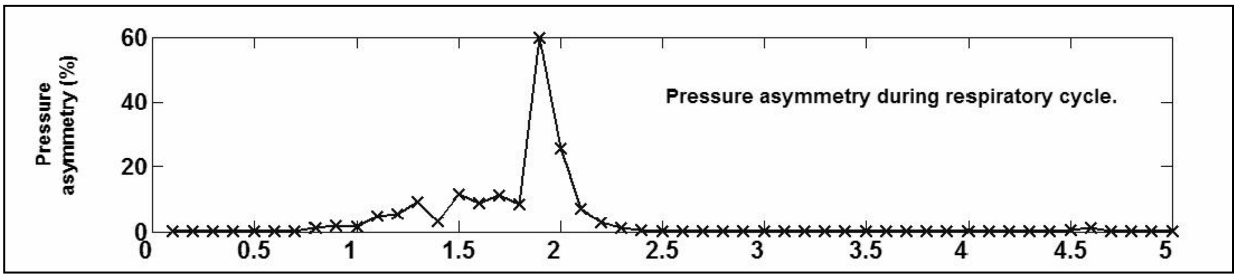

Figure 9: Pressure asymmetry during one ventilation cycle. High asymmetry exists during inspiration. During expiration, pressures are identical at each tree-end.

4.3 Three Generations Lung Model

All preceding simulations use theoretical models of lung geometry. Now that flow structure in a tree is better understood, it is interesting to work with a more realistic modelisation of the lung. The geometrical model used in this section is a part of the numerical lung built by H. Kitaoka [4]. Only the three first generations are used here and piston structures are added at each outlets, see the tree on Fig. 10. The tree has no more symmetry properties and pistons now pump quantity of air corresponding to the volume they must feed. They are synchronously oscillating in time, with more realistic ventilation: inspiration time is 2 seconds long and expiration time is 3 seconds long. The normalized amplitude of the pistons is shown on the right part of Fig. 10.

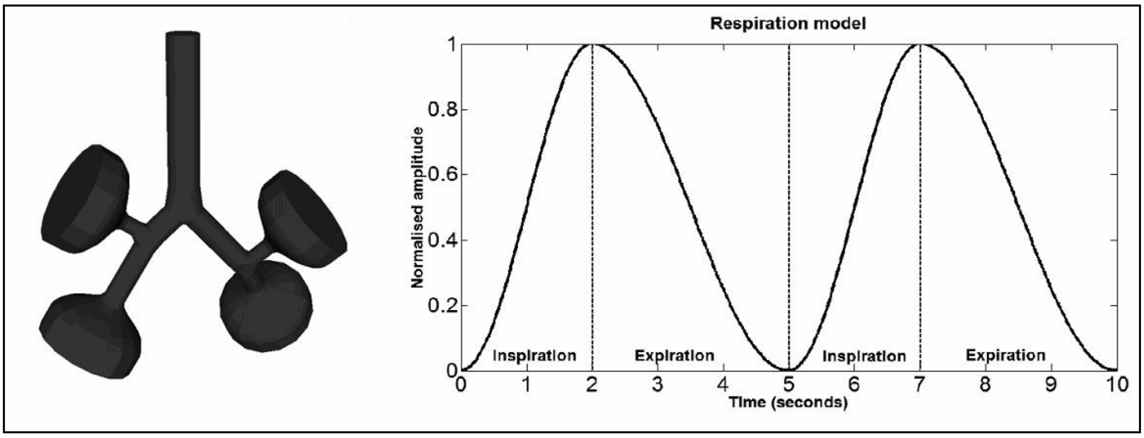

Figure 10: Left: tree used in this section, it is completely asymmetric. Right: normalized pistons amplitude, with 2 seconds inspiration and 3 seconds expiration.

Velocity amplitudes at maximum inspiration rate are shown on Fig. 11. The left part corresponds to inspiration. M-shapes are visible as before. However, these shapes are now linked to two effects which are working together to create this typical flow profile. Firstly, according to the observations in the preceding theoretical models, we know that inertia creates a M-shape in the second generation. Its high velocity region is oriented towards the branch which is better aligned with the trachea. Moreover, this last type of branch is, in the case of the lung, the most flow demanding branches. Hence, its piston will pump more and will create a deformation of the velocity profile to fit this demand. What is remarkable is that inertial effects and flow demand are in some way coordinated in real lung. This coordination implies lower pressure gradients in all four pistons than in any other configuration and hence lower energy costs. This could be the result of natural selection, which could have favoured lungs inspiring in a way that takes into account inertial effects, in order to minimize ventilation costs.

On the right part of Fig. 11 are represented expiratory velocity amplitudes at maximum expiration rate. Maximum velocity during expiration is lower than maximum velocity during inspiration because of the longest expiration time. This implies that inertial effects will always be smaller during expiration than during inspiration. This observation associated with the property that expiratory flow is more homogenous, leads to the conclusion that expiration seems easier to activate. This could be a part of the explanation to why inspiration is always active (muscles create the movement) while expiration could be passive (at rest, elastic forces are sufficient to create the movement).

Hence, inspiration and expiration are completely different phenomena. This difference is also visible in the way lung is functioning. Natural selection has probably favoured lungs which are adapted to inspiratory inertial effects. Moreover, our calculations have lead to a better understanding to why expiration can be passive while inspiration is always active.

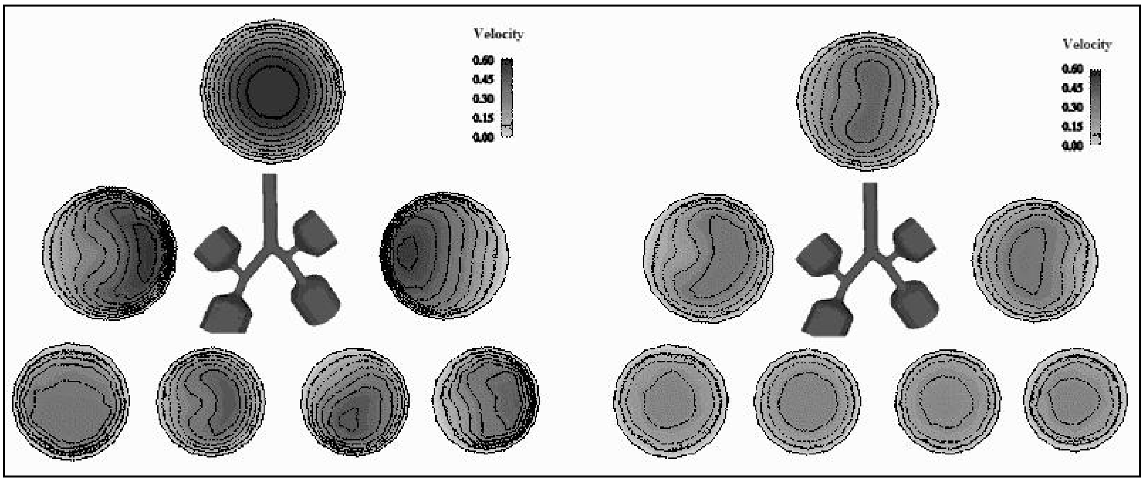

Figure 11: Left: velocities amplitude during inspiration (maximum velocities time). Profile in the second generation is the consequence of two effects: inertia and asymmetric pumping of the pistons. Right: velocities amplitude during expiration (maximum velocities time), flow is more homogenous than during inspiration.

5 Discussion

Although the lung is a very complicated system, numerical simulation can help us better understanding it through simplified theoretical models. Hence, it has been shown that inertial effects have great influence on flow in the lung, even at rest. The first observation is that inertial effects, and consequently flow profiles, are different during inspiration and expiration. Hence, during inspiration and without regulation, inertia prevents flow properties to be homogenous, in fact it leads to very few flow in some part of the structure while others are too much fed. This fact must have been taken into account by natural selection. For instance, evolution has probably favoured lungs which are pumping more flow towards its base, because of inspiratory inertial effects. On the contrary, inertial effects have less consequence on flow homogeneity during expiration. These differences have consequences on the mechanism of ventilation. Hence, inspiration, which is most inertia sensitive and should be more regulated, is always an active movement (muscles driven). On the contrary, expiration, leading to relatively homogenous flow, can be passive at low ventilation regime (elasticity forces).

There are many other applications of those calculations. For instance, particles tracing can be easily obtained and deposition sites can be predicted. Moreover, quantitative measures of Reynolds numbers along the tree have led to a generation threshold from where Poiseuille regime is sufficient to represent air circulation, problem which has been studied in [6]. With acinus and diffusion models like in [8], it will be then possible to stack the different levels of modelisation to obtain what can be called a “numerical lung”. Such a tool could be a great advantage for understanding lung structure or tracking lung disease.

References

[1] Weibel ER, The Pathway for Oxygen. Harvard University Press 1984.

[2] Mauroy B, Filoche M, Andrade Jr. JS, Sapoval B. Interplay between geometry and flow distribution in an airway tree. Physical Review Letters 2003; 90:148101 1-4.

[3] Schreck RM. Laminar flow through bifurcations with applications to the human lung 1972; Northwestern University thesis.

[4] Kitaoka H, Ryuji T, Suki B. A three-dimensional model of the human airway tree. J Appl Physiol 1999; 87: 2207-2217.

[5] Mauroy B, Filoche M, Andrade Jr. JS, Sapoval B. Reply to J.P. Butler and A. Tsuda. Physical Review Letters 2004; 93: 049802.

[6] Mauroy B, Filoche M, Weibel ER, Sapoval B. An optimal bronchial tree may be dangerous. Nature 2004; 427: 633-636.

[7] Mauroy B. Hydrodynamique dans le poumon, relations entre flux et géométries. Thesis from Ecole Normale Supérieure de Cachan 2004.

[8] Felici M, Filoche M, Sapoval B. Diffusional screening in the human pulmonary acinus. J Appl Physiol 2003; 94: 2010.